

## A five-variable refined plate theory for thermal buckling analysis of composite plates

Hussein A. Hashim\*<sup>1</sup> and Ibtehal Abbas Sadiq<sup>2</sup>

<sup>1</sup>Department of Mechanical Engineering, University of Baghdad, Wasit, Al- Jawadeen, Iraq

<sup>2</sup>Department of Mechanical Engineering, University of Baghdad, Baghdad, Al- Kadhimiya, Iraq

(Received March 30, 2021, Revised June 16, 2021, Accepted June 18, 2021)

**Abstract.** This research is devoted to investigate the thermal buckling analysis behaviour of laminated composite plates, by applying an analytical model based on a refined plate theory (RPT) with five independent unknown variables. The theory accounts for parabolic distribution of the transvers shear strains through the plate thickness, and satisfied the zero traction boundary condition on the surface without using shear correction factors, hence a shear correction factor is not required. The governing differential equations and associated boundary conditions are derived by employing the principle of virtual work and solved via Navier-type analytical procedure to obtain critical buckling temperature for simply supported boundary condition of symmetric and antisymmetric cross-ply and angle-ply laminated plates. MATLAB 2018 program is used to investigate the effect of thickness ratio ( $a/h$ ), aspect ratio ( $a/b$ ), orthogonality ratio ( $E_1/E_2$ ), coefficient of thermal expansion ratio ( $\alpha_2/\alpha_1$ ) and numbers of layers on thermal buckling of laminated plate. It can be concluded that this theory gives good results when compared with other theory.

**Keywords:** thermal buckling; cross & angle-ply plate; critical buckling temperature; refined plate theory

### 1. Introduction

Designs of airframes for high speed flight and spacecraft structures have to consider carefully the effect of the thermal environment on structural and material behavior. The plate structures are often subjected to severe thermal environments during launching and reentry and may have significant and unavoidable initial geometric imperfections. When the plate is subjected to temperature change, thermally induced compressive stresses are developed in the constraint plate due to thermoelastic properties and consequently buckling occurs. Therefore, the study of the buckling behavior of composite laminated plates under such environmental conditions is a matter of considerable importance in the design of aircraft. Thangaratnam and Ramachandran (1989) used finite element method using semiloof elements to analyse critical buckling temperature for composite laminates under thermal load. The equation of motion for critical temperature is obtained by equating the second variation of total potential energy to zero. Different boundary condition for cross-ply and angle-ply symmetric and antisymmetric plates. Chang and Leu (1991) studied thermal buckling of antisymmetric angle-ply laminated simply supported subjected to uniform thermal load using higher order deformation theory which account for transverse shear and transverse normal

---

\*Corresponding author, M.Sc. Student, E-mail: [H.ALzadi1803M@coeng.uobaghdad.edu.iq](mailto:H.ALzadi1803M@coeng.uobaghdad.edu.iq)

strain to obtain exact-closed form solution. Chen *et al.* (1991) studied the thermal buckling behavior of composite laminated plates subjected to uniform or non-uniform temperature fields are analyzed with the aid of the finite element method. Noor and Scott Burton (1992) presented three-dimensional analytical solution for thermal buckling multilayered angle-ply composite plates with temperature-dependent thermo elastic properties. The temperature is assumed to be independent of the surface coordinates, but has symmetric variation along plate thickness. Shu and Sun (1994) used a higher-order displacement field is developed for study the analysis of the thermomechanical buckling of composite plates subjected to thermal or mechanical load. Exact closed-form solutions of symmetric cross-ply laminates are obtained. Prabhu and Dhanaraj (1994) studied thermal buckling of laminated composite plates is analysed using the finite element method based on the Reissner-Mindlin first order shear deformation theory. The nine-node Lagrangian isoparametric element is employed for the thermal buckling analysis of symmetric cross-ply, anti-symmetric angle-ply and quasi-isotropic laminates subjected to uniform temperature distribution. Matsunaga (2006) investigated thermal buckling of angle-ply laminated composite and sandwich plates based on two-dimensional global higher order shear deformation theory. Abdul-Majeed *et al.* (2011) investigated thermal buckling of isotropic thermo elastic thin plates using governing differential equation and the Rayleigh-Ritz method. Three types of thermal distribution have been considered these are: uniform temperature, linear distribution and non-linear thermal distribution across thickness. Bourada *et al.* (2012) used a new four-variable refined plate theory for thermal buckling analysis of functionally graded material (FGM) sandwich plates. The thermal loads are assumed as uniform, linear, and nonlinear temperature rises across the thickness direction. Kumar *et al.* (2013) investigated the effect of temperature on the buckling response of a laminated composite plate subjected to thermo mechanical loadings. Mechanical loading consists of uniaxial, biaxial, and shear. The distribution of temperature on the surface is considered to be uniform. The mathematical formulation is based on higher order shear deformation theory. Jameel (2013) investigated critical buckling temperature of cross-ply and angle-ply composite laminated plate using classical laminated and higher order shear deformation plate theory. Equations of motion are solved using Navier and Levy methods for symmetric and anti-symmetric laminated plates. Kumar and Gupta (2014) investigated thermal buckling of symmetric cross-ply composite laminate using the classical laminated plate theory & first order shear deformation theory in conjunction with the Rayleigh-Ritz method is used for the evaluation of the thermal buckling parameters of structures made out of graphite fibres with an epoxy matrix. Symmetrically cross-ply laminated composite plates subjected to a combination of uniform temperature distribution through the thickness. Singh (2014) presented thermal buckling behavior of laminated composite curved panel embedded with shape memory alloy fiber based on higher order shear deformation plate theory. Variational principle with finite element modeling under uniform temperature loading is used to obtain the responses. Cetkovic (2016) Studied thermal buckling of laminated composite plates, based on Layer wise Theory of Reddy and new version of Layer wise Theory of Reddy. From the strong form, analytical solution is derived based on Navier's type, while the weak form is analysed using the isoperimetric finite element approximation. Ounis and Belarbi (2017) studied the thermal buckling behavior of laminated plates with rectangular cut outs using classical plate theory as a base for finite element method. Xing and Wang (2017) concerned the critical buckling temperature of functionally graded rectangular thin plates. Closed form solutions for the critical thermal parameter are obtained for the plate with different boundary conditions under uniform, linear and nonlinear temperature fields using separation-of-variable method. Hussein and Alasadi (2018) investigation of the stress-strain for E-glass fiber/polyester composite plates subjected to the uniform temperature at various factors, such as fiber volume

fraction and fiber orientation. using finite element solution. Sadiq and Majeed (2019) studied critical buckling temperature of angle-ply laminated plate is developed using a new higher-order displacement field. Equations of motion based on higher-order theory angle-ply plates are derived through Hamilton's principle, and solved using Navier-type solution to obtain critical buckling temperature for simply supported laminated plates. Tounsi *et al.* (2019) presented a novel higher-order shear deformation theory (HSDT) for buckling analysis of functionally graded plates. The present theory accounts for both shear deformation and thickness stretching effects by a parabolic variation of all displacements across the thickness, and satisfies the stress-free boundary conditions on the upper. The governing equations are obtained by the principle of virtual work. Analytical solutions for the buckling analyses are solved for simply supported sandwich plate. Belbachir *et al.* (2019). Investigated to describe the response of anti-symmetric cross-ply laminated plates subjected to a uniformly distributed nonlinear thermo-mechanical loading. By using refined plate theory. The undetermined integral terms are used and the variables number is reduced to four. The boundary conditions on the top and the bottom surfaces of the plate are satisfied. The principle of virtual work is used to obtain governing equations and boundary conditions. Navier solution for simply supported plates is used to derive analytical solutions. Abualnour *et al.* (2019). Studied The thermo-mechanical bending behavior of the antisymmetric cross-ply laminates is examined using a new simple four variable trigonometric plate theory. The proposed theory utilizes a novel displacement field which introduces undetermined integral terms and needs only four variables. Belbachir *et al.* (2020). Deals with the flexural analysis of anti-symmetric cross-ply laminated plates under nonlinear thermal loading using a refined plate theory with four variables. The undetermined integral terms are used and the number of variables is reduced to four. The principle of virtual work is used to obtain governing equations and boundary conditions. Navier solution for simply supported plates is used to derive analytical solutions. Abdul and Majeed (2020) a modified Fourier-Ritz approach for first time is used to study dynamic transverse response of laminated plates with different boundary conditions based on classical plate's theory. The transverse displacement component of the plate is represented by Fourier series which is modified by adding auxiliary functions to cosine series so as to accelerate the convergence of the series and the solution. Ghadimi (2020) studied stability functions are calculated to obtain critical elastic buckling loads of asymmetric and axisymmetric one-span non-sway bending frames made up of laminated thin beams and columns with through-thickness mechanical properties variation subjected to axial compression. The shear and axial deformations are neglected. It is assumed that the members are perfect and axial compression is applied to neutral axis without eccentricity. The relative rotations of beams with respect to columns are occurred due to semi-rigid connections at joints of the bending frame. Menasria *et al.* (2020) Presented dynamic analysis of the FG-sandwich plate seated on elastic foundation with various kinds of support using refined shear deformation theory. The zero-shear stresses at the free surfaces of the FG-sandwich plate are ensured without introducing any correction factors. The four equations of motion are determined via Hamilton' principle and solved by Galerkinw's approach for FG-sandwich plate with three kinds of the support. Chikr *et al.* (2020). Studied the buckling analysis of material sandwich plates based on a two-parameter elastic foundation under various boundary conditions is investigated on the basis of a new theory of refined trigonometric shear deformation. The governing equations and boundary conditions are obtained. Bensaid *et al.* (2021) investigate the static bending and buckling response of Functionally Graded (FG) nanobeams by employing a new refined first order shear deformation beam theory. The elegance of this novel theory is that, not only has one variable in terms of equations of motion as in classical beam theory (EBT) but also accounts for the effect of transverse shear deformation without any requirement of Shear Correction Factors

(SCFs). Tahir *et al.* (2021). Presented Wave propagation analysis of porous functionally graded (FG) sandwich plate in a hygro-thermal environment. By using a simple four-unknown integral higher-order shear deformation theory (HSDT). The effect of moisture and temperature on wave propagation in porous FG sandwich plates is investigated by considering their role on the material's expansion. Bakoura *et al.* (2021) Studied the mechanical buckling analysis of simply-supported functionally graded plates are carried out using a higher shear deformation theory (HSDT) in conjunction with the stress function method. Without using shear correction factor and gives rise to a variation of transverse shear stress such that the transverse shear stresses vary parabolically through the thickness satisfying the surface conditions without stress of shear.

In present work, critical temperature of simply supported composite cross-ply and angle-ply plate is obtained using refined five-parameter plate theory (RPT). The significant advantage of our proposed theory is that five unknown variable exists in its displacement formula and governing equation. The displacement  $u$  in  $x$  direction, the displacement  $v$  in  $y$  direction, the transverse displacement  $W$  contains three components of bending  $w_b$ , shear  $w_s$  and extension  $w_a$  which these components are function of coordinates  $x$  and  $y$ . the effect of thickness ratio ( $a/h$ ), aspect ratio( $a/b$ ), orthogonality ratio ( $E_1/E_2$ ), coefficient of thermal expansion ratio ( $\alpha_1/\alpha_2$ ) and numbers of layers on thermal buckling of laminated plate for symmetric and antisymmetric thin and thick plate are investigated.

## 2. Theoretical analysis

### 2.1 Displacement field

Consider a rectangular plate of total thickness ( $h$ ) composed on ( $n$ ) orthotropic layers with the coordinate system (see Fig. 1) Kim (2009). Refined plate theory satisfies equilibrium conditions at the top and bottom forces of the plate without using shear correction factor. The transverse displacement  $W$  includes three components of extension  $w_a$ , bending  $w_b$  and shear  $w_s$  the displacement field may be expressed as Kim (2009):

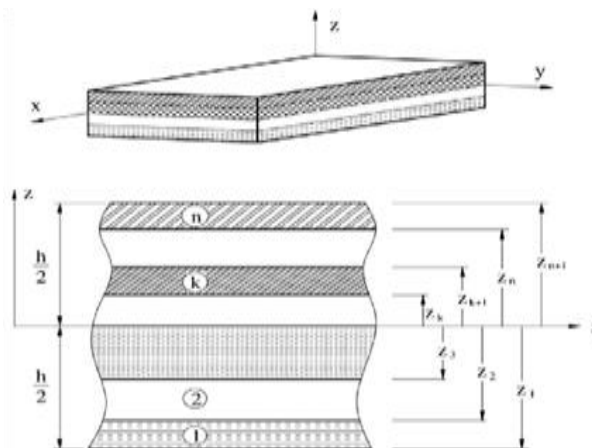


Fig. 1 Developed samples from stir casting

$$\begin{aligned}
 U(x, y, z) &= u(x, y) - z \left[ \frac{\partial w_b}{\partial x} \right] + z \left[ \frac{1}{4} - \frac{5}{3} \left( \frac{z}{h} \right)^2 \right] \frac{\partial w_s}{\partial x} \\
 V(x, y, z) &= v(x, y) - z \left[ \frac{\partial w_b}{\partial y} \right] + z \left[ \frac{1}{4} - \frac{5}{3} \left( \frac{z}{h} \right)^2 \right] \frac{\partial w_s}{\partial y} \\
 W(x, y, z) &= w_a(x, y) + w_b(x, y) + w_s(x, y)
 \end{aligned} \tag{1}$$

For small strain Linear, the strain-displacement relations take the form Reddy 2004.

$$\begin{aligned}
 \epsilon_x &= \frac{\partial u}{\partial x}, \quad \epsilon_y = \frac{\partial v}{\partial y} \\
 \epsilon_{xy} &= \frac{1}{2} \left( \frac{\partial u}{\partial y} + \frac{\partial v}{\partial x} \right) = \frac{1}{2} \gamma_{xy}, \quad \epsilon_{yz} = \frac{1}{2} \left( \frac{\partial v}{\partial z} + \frac{\partial w}{\partial y} \right) = \frac{1}{2} \gamma_{yz}, \quad \epsilon_{xz} = \frac{1}{2} \left( \frac{\partial u}{\partial z} + \frac{\partial w}{\partial x} \right) = \frac{1}{2} \gamma_{xz}
 \end{aligned} \tag{2}$$

The strain components will be derived, based on the displacement refined of plate, from Eq. (1) and (2) as:

$$\begin{aligned}
 \epsilon_x &= \frac{\partial u}{\partial x} - z \frac{\partial^2 w_b}{\partial x^2} + z \left[ \frac{1}{4} - \frac{5}{3} \left( \frac{z}{h} \right)^2 \right] \frac{\partial^2 w_s}{\partial x^2}, \quad \epsilon_y = \frac{\partial v}{\partial y} - z \frac{\partial^2 w_b}{\partial y^2} + z \left[ \frac{1}{4} - \frac{5}{3} \left( \frac{z}{h} \right)^2 \right] \frac{\partial^2 w_s}{\partial y^2} \\
 \gamma_{xy} &= \frac{\partial u}{\partial y} + \frac{\partial v}{\partial x} - 2z \left( \frac{\partial^2 w_b}{\partial x \partial y} \right) + 2z \left[ \frac{1}{4} - \frac{5}{3} \left( \frac{z}{h} \right)^2 \right] \frac{\partial^2 w_s}{\partial x \partial y}, \\
 \gamma_{yz} &= \frac{\partial w_a}{\partial y} + \left[ \frac{5}{4} - 5 \left( \frac{z}{h} \right)^2 \right] \frac{\partial w_s}{\partial y}, \quad \gamma_{xz} = \frac{\partial w_a}{\partial x} + \left[ \frac{5}{4} - 5 \left( \frac{z}{h} \right)^2 \right] \frac{\partial w_s}{\partial x}
 \end{aligned} \tag{3}$$

The strains associated with the displacements are:

$$\begin{aligned}
 \epsilon_x &= \epsilon_x^0 + z k_x^b + f k_x^s, \quad \epsilon_y = \epsilon_y^0 + z k_y^b + f k_y^s, \quad \epsilon_z = 0, \\
 \gamma_{xy} &= \gamma_{xy}^0 + z k_{xy}^b + f k_{xy}^s, \quad \gamma_{yz} = \gamma_{yz}^a + g \gamma_{yz}^s, \quad \gamma_{xz} = \gamma_{xz}^a + g \gamma_{xz}^s
 \end{aligned} \tag{4}$$

where:

$$\begin{aligned}
 \begin{Bmatrix} \epsilon_x^0 \\ \epsilon_y^0 \\ \gamma_{xy}^0 \end{Bmatrix} &= \begin{Bmatrix} \frac{\partial u}{\partial x} \\ \frac{\partial v}{\partial y} \\ \frac{\partial u}{\partial y} + \frac{\partial v}{\partial x} \end{Bmatrix}, \quad \begin{Bmatrix} k_x^b \\ k_y^b \\ k_{xy}^b \end{Bmatrix} = \begin{Bmatrix} -\frac{\partial^2 w_b}{\partial x^2} \\ -\frac{\partial^2 w_b}{\partial y^2} \\ -2 \frac{\partial^2 w_b}{\partial x \partial y} \end{Bmatrix}, \quad \begin{Bmatrix} k_x^s \\ k_y^s \\ k_{xy}^s \end{Bmatrix} = \begin{Bmatrix} -\frac{\partial^2 w_s}{\partial x^2} \\ -\frac{\partial^2 w_s}{\partial y^2} \\ -2 \frac{\partial^2 w_s}{\partial x \partial y} \end{Bmatrix} \\
 \begin{Bmatrix} \gamma_{xz}^a \\ \gamma_{yz}^a \end{Bmatrix} &= \begin{Bmatrix} \frac{\partial w_a}{\partial x} \\ \frac{\partial w_a}{\partial y} \end{Bmatrix}, \quad \begin{Bmatrix} \gamma_{xz}^s \\ \gamma_{yz}^s \end{Bmatrix} = \begin{Bmatrix} \frac{\partial w_s}{\partial x} \\ \frac{\partial w_s}{\partial y} \end{Bmatrix}, \quad f = -\frac{1}{4} z + \frac{5}{3} z \left( \frac{z}{h} \right)^2, \quad g = \frac{5}{4} - 5 \left( \frac{z}{h} \right)^2
 \end{aligned} \tag{5}$$

## 2.2 Hamilton's principle

Hamilton's principle is used herein to derive the equations of motion appropriate to the displacement field. The principle can be stated in analytical form as Reddy (2004).

$$0 = \int_0^T (\delta U + \delta V) dt \tag{6}$$

The strain energy  $\delta U$  can be written as:

$$\delta U = \int_V (\sigma_x \delta \mathcal{E}_x + \sigma_y \delta \mathcal{E}_y + \sigma_{xy} \delta \gamma_{xy} + \sigma_{yz} \delta \gamma_{yz} + \sigma_{xz} \delta \gamma_{xz}) dV \quad (7)$$

Substituting Eq. (4) into Eq. (7) we get:

$$\delta U = \int_V \left[ \sigma_{xx} (\delta \mathcal{E}_x^0 + z \delta k_x^b + f \delta k_x^s) + \sigma_{yy} (\delta \mathcal{E}_y^0 + z \delta k_y^b + f \delta k_y^s) \right. \\ \left. + \sigma_{xy} (\delta \gamma_{xy}^0 + z \delta k_{xy}^b + f \delta k_{xy}^s) + \sigma_{yz} (\delta \gamma_{yz}^a + g \delta \gamma_{yz}^s) + \sigma_{xz} (\delta \gamma_{xz}^a + g \delta \gamma_{xz}^s) \right] dV \quad (8)$$

$$\delta U = \int_A \left[ N_x \delta \mathcal{E}_x^0 + N_y \delta \mathcal{E}_y^0 + N_{xy} \delta \gamma_{xy}^0 + M_x^b \delta k_x^b + M_y^b \delta k_y^b + M_{xy}^b \delta k_{xy}^b + M_x^s \delta k_x^s \right. \\ \left. + M_y^s \delta k_y^s + M_{xy}^s \delta k_{xy}^s + Q_{yz}^a \delta \gamma_{yz}^a + Q_{xz}^a \delta \gamma_{xz}^a + Q_{yz}^s \delta \gamma_{yz}^s + Q_{xz}^s \delta \gamma_{xz}^s \right] dx dy$$

where:

$$(N_x, N_y, N_{xy}) = \int_{-\frac{h}{2}}^{\frac{h}{2}} (\sigma_x, \sigma_y, \sigma_{xy}) dz = \sum_{k=1}^N \int_{z_k}^{z_{k+1}} (\sigma_x, \sigma_y, \sigma_{xy}) dz$$

$$(M_x^b, M_y^b, M_{xy}^b) = \int_{-\frac{h}{2}}^{\frac{h}{2}} (\sigma_x, \sigma_y, \sigma_{xy}) z dz = \sum_{k=1}^N \int_{z_k}^{z_{k+1}} (\sigma_x, \sigma_y, \sigma_{xy}) z dz \quad (9)$$

$$(M_x^s, M_y^s, M_{xy}^s) = \int_{-\frac{h}{2}}^{\frac{h}{2}} (\sigma_x, \sigma_y, \sigma_{xy}) f dz = \sum_{k=1}^N \int_{z_k}^{z_{k+1}} (\sigma_x, \sigma_y, \sigma_{xy}) f dz$$

$$(Q_{xz}^a, Q_{yz}^a, Q_{xz}^s, Q_{yz}^s) = \int_{-\frac{h}{2}}^{\frac{h}{2}} (\sigma_{xz}, \sigma_{yz}, g \sigma_{xz}, g \sigma_{yz}) dz = \sum_{k=1}^N \int_{z_k}^{z_{k+1}} (\sigma_{xz}, \sigma_{yz}, g \sigma_{xz}, g \sigma_{yz}) dz$$

Substituting Eq. (5) in Eq. (8) and by using by parts integrating we get the final strain energy as below:

$$\delta U = - \int_A \left[ \begin{array}{l} \frac{\partial N_x}{\partial x} \delta u + \frac{\partial N_y}{\partial y} \delta v + \frac{\partial N_{xy}}{\partial y} \delta u + \frac{\partial N_{xy}}{\partial x} \delta v + \frac{\partial^2 M_x^b}{\partial x^2} \delta w_b \\ + \frac{\partial^2 M_y^b}{\partial y^2} \delta w_b + 2 \frac{\partial^2 M_{xy}^b}{\partial x \partial y} \delta w_b + \frac{\partial^2 M_x^s}{\partial x^2} \delta w_s + \frac{\partial^2 M_y^s}{\partial y^2} \delta w_s \\ + 2 \frac{\partial^2 M_{xy}^s}{\partial x \partial y} \delta w_s + \frac{\partial Q_{yz}^a}{\partial y} \delta w_a + \frac{\partial Q_{xz}^a}{\partial x} \delta w_a + \frac{\partial Q_{yz}^s}{\partial y} \delta w_s + \frac{\partial Q_{xz}^s}{\partial x} \delta w_s \end{array} \right] dx dy \quad (10)$$

The Work done by applied thermal Forces can be written as:

$$\delta V = \int_A \left[ N_x^T \frac{\partial^2 (w_a + w_b + w_s)}{\partial x^2} + N_y^T \frac{\partial^2 (w_a + w_b + w_s)}{\partial y^2} + 2 N_{xy}^T \frac{\partial^2 (w_a + w_b + w_s)}{\partial x \partial y} \right] dA \quad (11)$$

### 2.3 Equation of motion

Substituting Eqs. (10)-(11) into Eq. (6) and then collecting the coefficient of  $(\delta u, \delta v, \delta w_a, \delta w_b$  and  $\delta w_s)$  to zero separately, the equation of motion for the ply plate are obtained as follows:

$$\delta u: \frac{\partial N_x}{\partial x} + \frac{\partial N_{xy}}{\partial y} = 0 \quad , \quad \delta v: \frac{\partial N_y}{\partial y} + \frac{\partial N_{xy}}{\partial x} = 0 \quad (12)$$

$$\delta w_a: \frac{\partial Q_{xz}^a}{\partial x} + \frac{\partial Q_{yz}^a}{\partial y} + N^T(\omega) = 0, \quad \delta w_b: \frac{\partial^2 M_x^b}{\partial x^2} + \frac{\partial^2 M_y^b}{\partial y^2} + 2 \frac{\partial^2 M_{xy}^b}{\partial x \partial y} + N^T(\omega) = 0$$

$$\delta w_s: \frac{\partial^2 M_x^s}{\partial x^2} + \frac{\partial^2 M_y^s}{\partial y^2} + 2 \frac{\partial^2 M_{xy}^s}{\partial x \partial y} + \frac{\partial Q_{xz}^s}{\partial x} + \frac{\partial Q_{yz}^s}{\partial y} + N^T(\omega) = 0$$

where:

$$N^T(\omega) = N_x^T \frac{\partial^2 (w_a + w_b + w_s)}{\partial x^2} + N_y^T \frac{\partial^2 (w_a + w_b + w_s)}{\partial y^2} + 2N_{xy}^T \frac{\partial^2 (w_a + w_b + w_s)}{\partial x \partial y}$$

The transformed stress-strain relations of an orthotropic lamina in a plane state of stress are Reddy (2004)

$$\begin{Bmatrix} \sigma_x \\ \sigma_y \\ \sigma_{xy} \end{Bmatrix} = \begin{bmatrix} \bar{Q}_{11} & \bar{Q}_{12} & \bar{Q}_{16} \\ \bar{Q}_{12} & \bar{Q}_{22} & \bar{Q}_{26} \\ \bar{Q}_{16} & \bar{Q}_{26} & \bar{Q}_{66} \end{bmatrix} \left( \begin{Bmatrix} \varepsilon_x \\ \varepsilon_y \\ \gamma_{xy} \end{Bmatrix} - \begin{Bmatrix} \alpha_{xx} \\ \alpha_{yy} \\ 2\alpha_{xy} \end{Bmatrix} \Delta T \right), \quad \begin{Bmatrix} \sigma_{yz} \\ \sigma_{xz} \end{Bmatrix} = \begin{bmatrix} \bar{Q}_{44} & \bar{Q}_{45} \\ \bar{Q}_{45} & \bar{Q}_{55} \end{bmatrix} \begin{Bmatrix} \gamma_{yz} \\ \gamma_{xz} \end{Bmatrix} \quad (13)$$

The force results are:

$$\begin{Bmatrix} \begin{Bmatrix} N_x \\ N_y \\ N_{xy} \end{Bmatrix} \\ \begin{Bmatrix} M_x^b \\ M_y^b \\ M_{xy}^b \end{Bmatrix} \\ \begin{Bmatrix} M_x^s \\ M_y^s \\ M_{xy}^s \end{Bmatrix} \end{Bmatrix} = \begin{bmatrix} A_{11} & A_{12} & A_{16} & B_{11} & B_{12} & B_{16} & B_{11}^s & B_{12}^s & B_{16}^s \\ A_{12} & A_{22} & A_{26} & B_{12} & B_{22} & B_{26} & B_{12}^s & B_{22}^s & B_{26}^s \\ A_{16} & A_{26} & A_{66} & B_{16} & B_{26} & B_{66} & B_{16}^s & B_{26}^s & B_{66}^s \\ B_{11} & B_{12} & B_{16} & D_{11} & D_{12} & D_{16} & D_{11}^s & D_{12}^s & D_{16}^s \\ B_{12} & B_{22} & B_{26} & D_{12} & D_{22} & D_{26} & D_{12}^s & D_{22}^s & D_{26}^s \\ B_{16} & B_{26} & B_{66} & D_{16} & D_{26} & D_{66} & D_{16}^s & D_{26}^s & D_{66}^s \\ B_{11}^s & B_{12}^s & B_{16}^s & D_{11}^s & D_{12}^s & D_{16}^s & H_{11}^s & H_{12}^s & H_{16}^s \\ B_{12}^s & B_{22}^s & B_{26}^s & D_{12}^s & D_{22}^s & D_{26}^s & H_{12}^s & H_{22}^s & H_{26}^s \\ B_{16}^s & B_{26}^s & B_{66}^s & D_{16}^s & D_{26}^s & D_{66}^s & H_{16}^s & H_{26}^s & H_{66}^s \end{bmatrix} \begin{Bmatrix} \varepsilon_x^0 \\ \varepsilon_y^0 \\ \gamma_{xy}^0 \\ k_x^b \\ k_y^b \\ k_{xy}^b \\ k_x^s \\ k_y^s \\ k_{xy}^s \end{Bmatrix} \begin{Bmatrix} Q_{yz}^a \\ Q_{xz}^a \\ Q_{yz}^s \\ Q_{xz}^s \end{Bmatrix} \quad (14)$$

$$= \begin{bmatrix} A_{11} & A_{11} & A_{44}^a & A_{45}^a \\ A_{11} & A_{11} & A_{45}^a & A_{55}^a \\ A_{44}^a & A_{45}^a & A_{44}^s & A_{45}^s \\ A_{45}^a & A_{55}^a & A_{45}^s & A_{55}^s \end{bmatrix} \begin{Bmatrix} \gamma_{yz}^a \\ \gamma_{xz}^a \\ \gamma_{yz}^s \\ \gamma_{xz}^s \end{Bmatrix} \begin{Bmatrix} N_x^T \\ N_y^T \\ N_{xy}^T \end{Bmatrix} = \sum_{k=1}^N \int_{z_k}^{z_{k+1}} \begin{bmatrix} \bar{Q}_{11} & \bar{Q}_{12} & \bar{Q}_{16} \\ \bar{Q}_{12} & \bar{Q}_{22} & \bar{Q}_{26} \\ \bar{Q}_{16} & \bar{Q}_{26} & \bar{Q}_{66} \end{bmatrix} \begin{Bmatrix} \alpha_{xx} \\ \alpha_{yy} \\ 2\alpha_{xy} \end{Bmatrix} \Delta T dz$$

where:

$$\alpha_{xx} = \alpha_1 \cos^2 \theta + \alpha_2 \sin^2 \theta, \quad \alpha_{yy} = \alpha_1 \sin^2 \theta + \alpha_2 \cos^2 \theta$$

$$2\alpha_{xy} = 2(\alpha_1 - \alpha_2) \sin \theta \cos \theta (A_{ij}, B_{ij}, D_{ij}, B_{ij}^s, D_{ij}^s, H_{ij}^s)$$

$$= \int_{-\frac{h}{2}}^{\frac{h}{2}} \bar{Q}_{ij}(1, z, z^2, f, zf, f^2) dz \quad (i, j = 1, 2, 6)$$

$$(A_{ij}, A_{ij}^a, A_{ij}^s) = \int_{-\frac{h}{2}}^{\frac{h}{2}} \bar{Q}_{ij}(1, g, g^2) dz \quad (i, j = 4, 5)$$

Eq. (12) can be expressed in terms of displacements ( $u, v, w_b, w_s, w_a$ ) by substituting for the stress resultants from Eq. (14). the equations of motion (12) take the form:

$$\begin{aligned}
& A_{11} \frac{\partial^2 u}{\partial x^2} + 2A_{16} \frac{\partial^2 u}{\partial x \partial y} + A_{66} \frac{\partial^2 u}{\partial y^2} + A_{16} \frac{\partial^2 v}{\partial x^2} + (A_{16} + A_{66}) \frac{\partial^2 v}{\partial x \partial y} + A_{26} \frac{\partial^2 v}{\partial y^2} \\
& - \left[ B_{11} \frac{\partial^3 w_b}{\partial x^3} + 3B_{16} \frac{\partial^3 w_b}{\partial x^2 \partial y} + (B_{12} + 2B_{66}) \frac{\partial^3 w_b}{\partial x \partial y^2} + B_{26} \frac{\partial^3 w_b}{\partial y^3} \right] \\
& - \left[ B_{11}^s \frac{\partial^3 w_s}{\partial x^3} + 3B_{16}^s \frac{\partial^3 w_s}{\partial x^2 \partial y} + (B_{12}^s + 2B_{66}^s) \frac{\partial^3 w_s}{\partial x \partial y^2} + B_{26}^s \frac{\partial^3 w_s}{\partial y^3} \right] = 0 \\
& A_{16} \frac{\partial^2 u}{\partial x^2} + (A_{12} + A_{66}) \frac{\partial^2 u}{\partial x \partial y} + A_{26} \frac{\partial^2 u}{\partial y^2} + A_{66} \frac{\partial^2 v}{\partial x^2} + 2A_{26} \frac{\partial^2 v}{\partial x \partial y} + A_{22} \frac{\partial^2 v}{\partial y^2} \\
& - \left[ B_{16} \frac{\partial^3 w_b}{\partial x^3} + (B_{12} + 2B_{66}) \frac{\partial^3 w_b}{\partial x^2 \partial y} + 3B_{26} \frac{\partial^3 w_b}{\partial x \partial y^2} + B_{22} \frac{\partial^3 w_b}{\partial y^3} \right] \\
& - \left[ B_{16}^s \frac{\partial^3 w_s}{\partial x^3} + (B_{12}^s + 2B_{66}^s) \frac{\partial^3 w_s}{\partial x^2 \partial y} + 3B_{26}^s \frac{\partial^3 w_s}{\partial x \partial y^2} + B_{22}^s \frac{\partial^3 w_s}{\partial y^3} \right] = 0 \\
& B_{11} \frac{\partial^3 u}{\partial x^3} + 3B_{16} \frac{\partial^3 u}{\partial x^2 \partial y} + (B_{12} + 2B_{66}) \frac{\partial^3 u}{\partial x \partial y^2} + B_{26} \frac{\partial^3 u}{\partial y^3} + B_{16} \frac{\partial^3 v}{\partial x^3} \\
& + (B_{12} + 2B_{66}) \frac{\partial^3 v}{\partial x^2 \partial y} + 3B_{26} \frac{\partial^3 v}{\partial x \partial y^2} + B_{22} \frac{\partial^3 v}{\partial y^3} \\
& - \left[ D_{11} \frac{\partial^4 w_b}{\partial x^4} + 4D_{16} \frac{\partial^4 w_b}{\partial x^3 \partial y} + 2(D_{12} + 2D_{66}) \frac{\partial^4 w_b}{\partial x^2 \partial y^2} + 4D_{26} \frac{\partial^4 w_b}{\partial x \partial y^3} + D_{22} \frac{\partial^4 w_b}{\partial y^4} \right] \\
& - \left[ D_{11}^s \frac{\partial^4 w_s}{\partial x^4} + 4D_{16}^s \frac{\partial^4 w_s}{\partial x^3 \partial y} + 2(D_{12}^s + 2D_{66}^s) \frac{\partial^4 w_s}{\partial x^2 \partial y^2} + 4D_{26}^s \frac{\partial^4 w_s}{\partial x \partial y^3} + D_{22}^s \frac{\partial^4 w_s}{\partial y^4} \right] \\
& + N^T(\omega) = 0
\end{aligned} \tag{15}$$

$$\begin{aligned}
& B_{11}^s \frac{\partial^3 u}{\partial x^3} + 3B_{16}^s \frac{\partial^3 u}{\partial x^2 \partial y} + (B_{12}^s + 2B_{66}^s) \frac{\partial^3 u}{\partial x \partial y^2} + B_{26}^s \frac{\partial^3 u}{\partial y^3} + B_{16}^s \frac{\partial^3 v}{\partial x^3} \\
& + (B_{12}^s + 2B_{66}^s) \frac{\partial^3 v}{\partial x^2 \partial y} + 3B_{26}^s \frac{\partial^3 v}{\partial x \partial y^2} + B_{22}^s \frac{\partial^3 v}{\partial y^3} \\
& - \left[ D_{11}^s \frac{\partial^4 w_b}{\partial x^4} + 4D_{16}^s \frac{\partial^4 w_b}{\partial x^3 \partial y} + 2(D_{12}^s + 2D_{66}^s) \frac{\partial^4 w_b}{\partial x^2 \partial y^2} + 4D_{26}^s \frac{\partial^4 w_b}{\partial x \partial y^3} + D_{22}^s \frac{\partial^4 w_b}{\partial y^4} \right] \\
& - \left[ H_{11}^s \frac{\partial^4 w_s}{\partial x^4} + 4H_{16}^s \frac{\partial^4 w_s}{\partial x^3 \partial y} + 2(H_{12}^s + 2H_{66}^s) \frac{\partial^4 w_s}{\partial x^2 \partial y^2} + 4H_{26}^s \frac{\partial^4 w_s}{\partial x \partial y^3} + H_{22}^s \frac{\partial^4 w_s}{\partial y^4} \right] \\
& + A_{55}^a \frac{\partial^2 w_a}{\partial x^2} + A_{44}^a \frac{\partial^2 w_a}{\partial y^2} + 2A_{45}^a \frac{\partial^2 w_a}{\partial x \partial y} + A_{55}^s \frac{\partial^2 w_s}{\partial x^2} + A_{44}^s \frac{\partial^2 w_s}{\partial y^2} + 2A_{45}^s \frac{\partial^2 w_s}{\partial x \partial y} + N^T(\omega) = 0 \\
& A_{55} \frac{\partial^2 w_a}{\partial x^2} + A_{44} \frac{\partial^2 w_a}{\partial y^2} + 2A_{45} \frac{\partial^2 w_a}{\partial x \partial y} + A_{55}^a \frac{\partial^2 w_s}{\partial x^2} + A_{44}^a \frac{\partial^2 w_s}{\partial y^2} + 2A_{45}^a \frac{\partial^2 w_s}{\partial x \partial y} + N^T(\omega) = 0
\end{aligned}$$

## 2.4 Navier Solution

In Navier's method the generalized displacements are expanded a double trigonometric series in terms of unknown parameters. The choice of function in the series is restricted to those which satisfy the boundary condition of problem. The Navier method is employed to obtain the closed form solutions of the partial differential equations in Eq. (12) for simply supported rectangular plates. Two types of simply supported boundary conditions are Reddy (2004).

**2.4.1 Navier solution of cross-ply laminated plates**

Assuming the following displacements form to satisfied simply supported boundary conditions for cross-ply

$$\begin{aligned}
 u &= \sum_{m=1}^{\infty} \sum_{n=1}^{\infty} U_{mn} \cos \alpha x \sin \beta y \\
 v &= \sum_{m=1}^{\infty} \sum_{n=1}^{\infty} V_{mn} \sin \alpha x \cos \beta y \\
 W_b &= \sum_{m=1}^{\infty} \sum_{n=1}^{\infty} W_{bmn} \sin \alpha x \sin \beta y \\
 W_s &= \sum_{m=1}^{\infty} \sum_{n=1}^{\infty} W_{smn} \sin \alpha x \sin \beta y \\
 W_a &= \sum_{m=1}^{\infty} \sum_{n=1}^{\infty} W_{amn} \sin \alpha x \sin \beta y
 \end{aligned} \tag{16}$$

**2.4.2 Navier solution of angle-ply laminated plates**

Assuming the following displacements form to satisfied simply supported boundary conditions for Angle-ply

$$\begin{aligned}
 u &= \sum_{m=1}^{\infty} \sum_{n=1}^{\infty} U_{mn} \sin \alpha x \cos \beta y \\
 v &= \sum_{m=1}^{\infty} \sum_{n=1}^{\infty} V_{mn} \cos \alpha x \sin \beta y \\
 W_b &= \sum_{m=1}^{\infty} \sum_{n=1}^{\infty} W_{bmn} \sin \alpha x \sin \beta y \\
 W_s &= \sum_{m=1}^{\infty} \sum_{n=1}^{\infty} W_{smn} \sin \alpha x \sin \beta y \\
 W_a &= \sum_{m=1}^{\infty} \sum_{n=1}^{\infty} W_{amn} \sin \alpha x \sin \beta y
 \end{aligned} \tag{17}$$

Substituting Eq. (16) and Eq. (17) into Eq. (15), the Navier solution of cross and Angle-ply laminates can be determined from Matrix stiffness Eq. (18):

$$\begin{bmatrix}
 s_{11} & s_{12} & s_{13} & s_{14} & 0 \\
 s_{12} & s_{22} & s_{23} & s_{24} & 0 \\
 s_{13} & s_{23} & s_{33} - k & s_{34} - k & -k \\
 s_{14} & s_{24} & s_{34} - k & s_{44} - k & s_{45} - k \\
 0 & 0 & -k & s_{45} - k & s_{55} - k
 \end{bmatrix}
 \begin{Bmatrix}
 U_{mn} \\
 V_{mn} \\
 W_{bmn} \\
 W_{smn} \\
 W_{amn}
 \end{Bmatrix}
 = 0 \tag{18}$$

where  $K = (N_x^T \alpha^2 + N_y^T \beta^2)$  and  $s_{ij}$  is the element of stiffness.

**3. Numerical results and discussion**

Using above analytical solutions of the refined plate theory based on displacement field. a computer program is built using MATLAB18 programming for thermal buckling of laminated cross ply and angle ply composite plates. The parametric effect of side to thickness ration ( $a/h$ ), aspect ratio ( $a/b$ ), modulus ratio ( $E_1/E_2$ ) and thermal expansion coefficient ratio ( $\alpha_2/\alpha_1$ ) on critical buckling temperature of laminated composite plates are analysed. The results obtained by RPT are compared with other different theories those of the refine four parameters plate theory (RPT), FSDT, HSDT, LWT an Noor, 1992.

Table 1 A critical temperature of cross-ply (0/90/90/0) simply supported square plate ( $a/b = 1$ )

a/h	Present	LWT <sup>1</sup>	FSDT <sup>2</sup>	HSDT <sup>3</sup>	HSDT <sup>4</sup>	GRT <sup>5</sup>			
						RPT	P = 3 (TOT)	P = 5	P = 7
4	0.06652	0.0514	0.0613	0.0570	0.0554	0.0711	0.05580	0.05888	0.06109
10	0.1658	0.1400	0.1598	0.1479	0.1436	0.1749	0.14784	0.15344	0.15704
20	0.2121	0.1976	/	0.2088	/	/	/	/	/
50	0.23029	0.2245	/	0.2383	/	/	/	/	/
100	0.2331	0.2291	0.2438	0.2432	0.2431	0.2440	0.24331	0.24378	0.24359

<sup>1</sup>Cetkovic (2016); <sup>2</sup>Shukla (2001); <sup>3</sup>Singh (2013); <sup>4</sup>Shu and Sun (1994); <sup>5</sup>Mansouri and Shariyat (2014)

Table 2 Dimensionless buckling temperature ( $T_{cr} a^2 h / \pi^2 D_{22}$ ) of cross-ply (0/90)<sub>N</sub> simply supported square plate

Lay-up	a/h	present	TOT <sup>1</sup>	RPT	Present DQ results (11*11)		
					P = 3(TOT)	P = 5	P = 7
(0/90) <sub>s</sub>	4	0.06652	0.0575	0.07115	0.05580	0.05888	0.06109
	10	0.165814	0.1522	0.17492	0.14784	0.15344	0.15704
	100	0.233139	0.2435	0.24405	0.24331	0.24348	0.24359
(0/90) <sub>2s</sub>	4	0.031579	0.0315	0.03348	0.03179	0.03205	0.03261
	10	0.078715	0.0797	0.08231	0.07963	0.08021	0.08081
	100	0.1106759	0.1148	0.11485	0.11478	0.11479	0.11481
(0/90) <sub>5s</sub>	4	0.02401	0.0247	0.02541	0.02521	0.02526	0.02562
	10	0.05985	0.0621	0.06247	0.06216	0.06250	0.06293
	100	0.0841534	0.0872	0.08716	0.08715	0.08716	0.08717

<sup>1</sup>Shu and Sun (1994)

### 3.1 Cross-ply composite plates

#### 3.1.1 Verification of results

To verify the suggested above solution, obtained results are compared with the refined four parameters plate theory (RPT) and other higher order theories.

A critical temperature of cross-ply (0/90/90/0) simply supported square plate ( $a/b = 1$ ) subjected to uniform temperature rise is analysed as listed in Table 1. Material constants are given as:

Material 1:  $\frac{E_1}{E_2} = 25$ ,  $E_2 = 1$ ,  $\frac{G_{12}}{E_2} = 0.5$ ,  $\frac{G_{13}}{E_2} = 0.5$ ,  $\frac{G_{23}}{E_2} = 0.2$ ,  $\nu_{12} = \nu_{13} = \nu_{23} = 0.25$ ,  $\frac{\alpha_2}{\alpha_1} = 3$ ,  $\alpha_1 = 1$

The critical temperature is normalized in the following form  $T_{cr} = \left( \frac{a^2 h}{\pi^2 D_{22}} * T \right)$ . Result show that while present model of refined plate theory utilized more displacement parameters (five parameters), it is generally more accurate result than (RPT) and less accurate than higher other order theories. Table 2. Show the effect of number of layers on critical temperature for different thickness ratio. Obtained result compared with other theory and give good agreement, increasing number of layers

Table 3 A critical temperature of cross-ply (0/90) simply supported square plate ( $a/b = 1$ )

theory	a/h							
	2	10/3	4	5	20/3	10	20	100
Present	0.2865	0.1922	0.1572	0.1179	0.07656	0.03828	0.01035	0.4249e-3
LWT <sup>1</sup>	0.3695	0.2391	0.1926	0.1419	0.09052	0.04449	0.01188	0.4858e-3
HSDT <sup>2</sup>	0.3198	0.2114	0.1729	0.1302	0.08524	0.04310	0.01177	0.4856e-3

<sup>1</sup>Cetkovic (2016), <sup>2</sup>Matsunaga (2005)

Table 4 A critical temperature of cross-ply (0/90/0) simply supported square plate ( $a/b = 1$ )

theory	a/h							
	2	10/3	4	5	20/3	10	20	100
Present	0.2945	0.2311	0.2033	0.1671	0.1206	0.0659	0.0191	8.0678e-4
LWT <sup>1</sup>	0.3595	0.2625	0.2272	0.1848	0.1340	0.07628	0.02316	0.9964e-3
NoorAK,3D <sup>2</sup>	/	/	0.2140	0.1763	/	0.07467	0.02308	0.9961e-3

<sup>1</sup>Cetkovic (2016), <sup>2</sup>Noor, 3D, <sup>3</sup>Matsunaga (2005), <sup>4</sup>Singh (2013)

Table 5 Effect ( $\alpha_2/\alpha_1$ ) on critical temperature of cross-ply (0/90/90/0) simply supported square plate ( $a/b = 1$ )

a/h	$T_{cr}$ ( $\alpha_2/\alpha_1$ )				
	2	4	6	8	10
5	0.09357	0.0851	0.07806	0.07208	0.06696
10	0.1741	0.1583	0.14519	0.13408	0.1245
15	0.2076	0.1888	0.1732	0.1599	0.14858
20	0.2227	0.2025	0.1858	0.1715	0.15937
50	0.2417	0.2199	0.2016	0.1862	0.17298
100	0.2447	0.2226	0.2041	0.18852	0.17512

Table 6 Critical temperature of symmetric and antisymmetric cross-ply  $[0/90]_N$  laminated thick and thin plates for different aspect ratio simply supported

Lay-up	a/h	$T_{cr}$ a/b			
		1	2	3	4
$[0/90]_s$	4	0.0665	0.07156	0.08053	0.08737
	10	0.1658	0.2019	0.2872	0.36024
	20	0.2122	0.2777	0.47497	0.70769
	100	0.2331	0.31608	0.6037	1.0376
$[0/90]_2$	4	0.0192	0.0252	0.0283	0.0301
	10	0.0455	0.09215	0.1268	0.1468
	20	0.0569	0.1542	0.2773	0.3799
	100	0.06189	0.19736	0.4558	0.8133

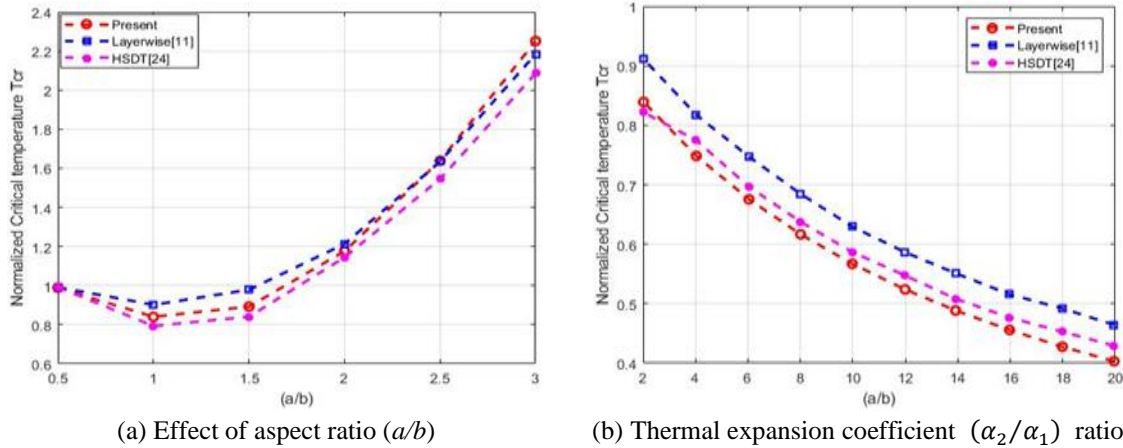


Fig. 1 Effect of aspect ratio ( $a/b$ ) and thermal expansion coefficient( $\alpha_2/\alpha_1$ ) ratio of cross-ply (0/90/90/0) Plate on critical buckling temperature  $T_{cr}$

caused decreasing critical temperature for all thickness ratio. Material used in this Table 2 is the same that use for Table 1.

Tables 3-4 show the effect of side to the thickness ratio ( $a/h$ ) on the critical temperature of cross-ply (0/90) and (0/90/0) simply supported square plate ( $a/b = 1$ ) subjected to uniform temperature respectively. Material properties for these tables as given as:

Material 2:  $\frac{E_L}{E_T} = 15, E_T = 1Gpa, \frac{G_{LT}}{E_T} = 0.5, \frac{G_{TT}}{E_T} = 0.3356, \nu_{LT} = 0.3, \nu_{TT} = 0.49, \frac{\alpha_L}{\alpha_0} = 0.015, \frac{\alpha_T}{\alpha_0} = 1, \alpha_0 = 10^{-6}$

Present results show that normalized critical temperature ( $T_{cr} = \alpha_0 T$ ) increase with the decrease of plate thickness and give good result for thick plate.

Fig. 1(a) present the effect aspect ratio with the variation of critical temperature for thin plate ( $a/h = 100$ ) simply supported plate for material 3 result of present model are compared with HSDT Kari RT, Palaninathan and Ramachandran (1989), and new layer wise Cetkovic (2016), and good agreement is achieved. Critical temperature increases with the increasing of ( $a/b$ ) ratio, after attaining its minimum value for ( $a/b = 1$ ).

### 3.1.2 Verification of results

The effect of ratio of thermal expansion coefficient ( $\alpha_2/\alpha_1$ ), on critical temperature is shown in Fig. 1(b), which show that critical temperature decreases, while ( $\alpha_2/\alpha_1$ ) increase. The material properties are given as:

Material 3:  $\frac{E_1}{E_2} = 20, E_2 = 1, \frac{G_{12}}{E_2} = 0.5, \frac{G_{13}}{E_2} = 0.5, \frac{G_{23}}{E_2} = 0.5, \nu_{12} = \nu_{13} = \nu_{23} = 0.25, \frac{\alpha_2}{\alpha_1} = 2, \alpha_1 = 0.1 \times 10^{-5}$

Table 5 show the effect of changing ( $\alpha_2/\alpha_1$ ) on critical temperature for four symmetric cross-ply (0/90/90/0) plates for different thickness ratio ( $a/h$ ), since stiffness increase when increasing orthotropic ratio therefore normalized critical temperature increase. The mechanical properties are the same in Table 1.

Changing of aspect ratio ( $a/h$ ) effect on critical buckling temperature of four symmetric and antisymmetric cross-ply (0/90/90/0) laminated thick and thin plates, are listed in Table 6. Which

Table 7 Effect ( $E_1/E_2$ ) on critical temperature of symmetric and antisymmetric cross-ply  $[0/90]_N$  laminated thick and thin plates simply supported

Lay-up	$E_1/E_2$	$T_{cr}$ $a/h$			
		5	10	20	100
$[0/90]_s$	10	0.2341	0.3493	0.3988	0.4178
	20	0.1169	0.2048	0.2531	0.2737
	40	0.0469	0.0997	0.1400	0.1610
	50	0.0336	0.0761	0.1127	0.1333
$[0/90]_{2s}$	10	0.1322	0.1973	0.2253	0.2360
	20	0.0574	0.1006	0.1243	0.1345
	40	0.0210	0.0447	0.0627	0.0721
	50	0.0147	0.0334	0.0494	0.0585
$[0/90]_{5s}$	10	0.1048	0.1565	0.1787	0.1872
	20	0.0440	0.0771	0.0952	0.1031
	40	0.0158	0.0335	0.0471	0.0542
	50	0.0110	0.0250	0.0370	0.0438
$[0/90]_2$	10	0.0854	0.1246	0.1410	0.1471
	20	0.0349	0.0590	0.0715	0.0767
	40	0.0124	0.0253	0.0345	0.0390
	50	0.0087	0.0188	0.0269	0.0313
$[0/90]_5$	10	0.0910	0.1354	0.1544	0.1617
	20	0.0375	0.0654	0.0806	0.0871
	40	0.0133	0.0282	0.0395	0.0453
	50	0.0093	0.02100	0.0309	0.0365
$[0/90]_{10}$	10	0.0918	0.1370	0.1564	0.1638
	20	0.0379	0.0664	0.0819	0.0886
	40	0.0135	0.0286	0.0402	0.0462
	50	0.0094	0.02131	0.0315	0.0372

show that critical temperature increases as aspect ratio ( $a/b$ ) increases, also it increases with increasing ( $a/h$ ) ratio which effected critical temperature larger than ( $a/b$ ) ratio. The mechanical properties are the same in Table 1.

In Table 7. show the effect of changing ( $E_1/E_2$ ) on critical temperature for four, eight and twenty layers symmetric and antisymmetric cross-ply plates for different thickness ratio ( $a/h$ ), notice that normalized critical temperature increase when aspect ratio increase, also normalized critical temperature decrease when orthotropic ratio increasing for both cross-ply symmetric and antisymmetric laminated plates. Using the mechanical properties are the same in Table 1.

Figs. 2(a)-2(d) shows first four buckling modes of moderately thick plate ( $a/h = 10$ ) rectangular ( $a/b = 2$ ) simply supported laminated plate.

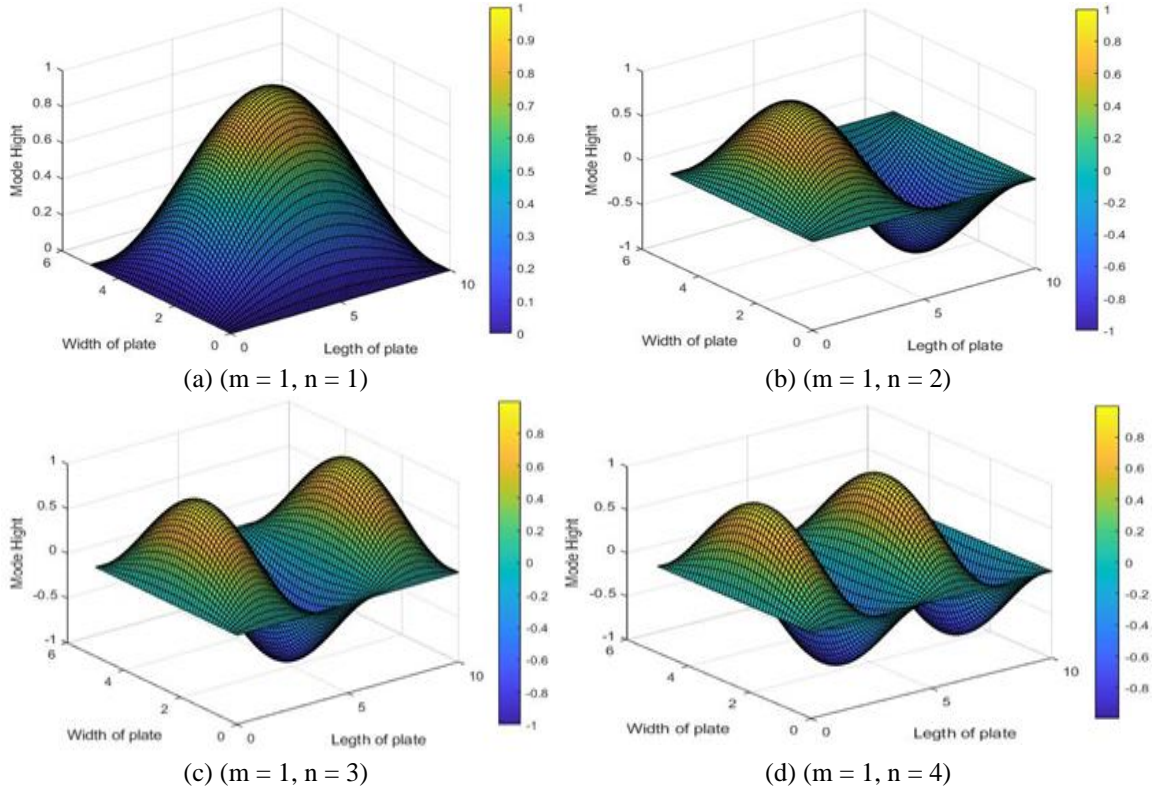


Fig. 2 Thermal buckling mode for symmetric cross-ply (0/90/90/0) square plate, No. of layers = 4,  $a/h = 10$ ,  $a/b = 1$

Table 8 A critical temperature ( $T_{cr} = \alpha_0 T$ ) of angle-ply (0/15/30/45) with simply supported square plate

a/h	References	$T_{cr}$			
		$\Theta = 0$ (m, n) (1,2)	$\Theta = 15$ (m, n) (1,2)	$\Theta = 30$ (m, n) (1,1)	$\Theta = 45$ (m, n) (1,1)
4	present	0.1973	0.2357	0.3081 (1, 2)	0.3200
	HODT	0.1872	0.2221	-	-
	Noor, 1992	0.1777	0.2087	-	-
	Discrepancy %	11	12.9	-	-
5	present	0.1591	0.1974	0.2596	0.2719
	HODT	0.1504	0.1849	0.2554 (1,2)	-
	Noor, 1992	0.1436	0.1753	0.2377 (1,2)	-
	Discrepancy %	10.7	12.6	9.2	-
10	present	0.06125	0.08478	0.11298	0.12247
	HODT	0.05917	0.08124	0.1125	0.12259
	Noor, 1992	0.05782	0.07904	0.1100	0.1194
	Discrepancy %	5.9	7.3	2.7	2.5

Table 8 Continued

a/h	References	$T_{cr}$			
		$\Theta = 0$ (m, n) (1,2)	$\Theta = 15$ (m, n) (1,2)	$\Theta = 30$ (m, n) (1,1)	$\Theta = 45$ (m, n) (1,1)
20	present	0.017728	0.0259	0.03477	0.038437
	HODT	0.01752	0.02552	0.03472	0.03844
	Noor, 1992	0.01739	0.02528	0.03446	0.03810
	Discrepancy %	1.9	2.4	0.9	0.88
100	present	0.0007469	0.001115	0.001502	0.001674
	HODT	0.0007465	0.001115	0.001502	0.001674
	Noor, 1992	0.0007463	0.001115	0.001502	0.001674
	Discrepancy %	0.08	0	0	0

Table 9 A critical temperature ( $T_{cr} = T * \alpha_0 * 10^3$ ) of antisymmetric six layers angle-ply (45/-45) with simply supported square plate ( $a/b = 1$ ) subjected to uniform temperature rise is analysed

a/h	Present	Chen and Liu, 1993	Discrepancy %
5	21.3428	21.3622	0.09
8	12.7245	12.7542	0.23
10	9.2833	9.2963	0.14
15	4.7908	4.7885	0.04
20	2.8564	2.8523	0.14
30	1.3264	1.3234	0.22
40	0.7580	0.7560	0.26
50	0.4887	0.4874	0.26
80	0.1924	0.1919	0.26
100	0.1234	0.1230	0.32

### 3.2 Angle-ply composite plate

#### 3.2.1 Verifications of results and design parameters

A critical temperature of antisymmetric angle-ply (0/15/30/45) with simply supported square plate ( $a/b = 1$ ) subjected to uniform temperature rise is analyzed. Material constants are given as: Material 4:  $\frac{E_1}{E_0} = 15, \frac{E_2}{E_0} = 1, \frac{G_{12}}{E_0} = \frac{G_{13}}{E_0} = 0.5, \frac{G_{23}}{E_0} = 0.3356, \nu_{12} = 0.3, \frac{\alpha_1}{\alpha_0} = 0.015, \frac{\alpha_2}{\alpha_0} = 1, E_0 = 1 \text{ Gpa}, \alpha_1 = 10^{-6}$ , No. of layer 10.

The critical temperature is normalized in the following form ( $T_{cr} = \alpha_0 T$ ). Table 8 presents the convergence analysis of non-dimensional critical temperature ( $T_{cr}$ ) of simply supported square plate for different side to thickness ratio ( $a/h$ ), which obtained results are compared with three dimensions elasticity theory proposed by Noor, (1992) which give good agreement with maximum discrepancy (12.9 %) for ten layers of antisymmetric angle-ply composite material.

A critical temperature of antisymmetric six layers angle-ply (45/-45) with simply supported square plate ( $a/b = 1$ ) subjected to uniform temperature rise is analyzed. Material constants are given as:

Material 5:  $E_1 = 21$ ,  $E_2 = E_3 = 1.7$ ,  $G_{12} = G_{13} = 0.65$ ,  $G_{23} = 0.639$ ,  $\nu_{12} = \nu_{13} = 0.21$ ,  $\alpha_2 = 16$ ,  $\alpha_1 = -0.21$ ,  $[45/-45]_3$

The critical temperature is normalized in the following form ( $T_{cr} = T\alpha_0 10^3$ ). Table 9 presents the convergence analysis of non-dimensional critical temperature ( $T_{cr}$ ) of simply supported square plate. which obtained results are compared with Chen and Liu, (1993), which give good agreement with maximum discrepancy (0.32 %) for six layers of antisymmetric angle-ply composite material.

Table 10 Normalized critical temperature [ $(T_{cr} = T * \alpha_1 * 10 * (b/h)^2$ )] for antisymmetric angle-ply plate  $a/h = 10$

b/a	Angle	No. Of layers	Present	Chen and Lui 1993	Discrepancy%
1	30	2	4.1527	4.0600	2.28
		4	7.0490	7.1345	1.19
		8	7.7179	7.7267	0.11
	45	2	4.3127	4.2070	2.5
		4	7.5512	7.6605	1.42
		8	8.2847	8.3010	0.19
	60	2	4.1527	4.0600	2.28
		4	7.0490	7.1345	1.19
		8	7.7179	7.7267	0.11
2	30	2	2.6865	2.6431	1.66
		4	4.9329	4.9757	0.86
		8	5.4537	5.4530	0.01
	45	2	2.5432	2.4942	1.96
		4	4.8633	4.8401	0.47
		8	5.4015	5.3240	1.45
	60	2	2.3776	2.3437	1.44
		4	4.3465	4.3038	0.87
		8	4.8148	4.7266	1.86

Table 11 Effects of Elastic moduli ratio on the dimensionless buckling temperature ( $T_{cr}\alpha_0 10^3$ ) of the square simply supported antisymmetric angle-ply  $(45/-45)_3$  plates ( $a/h = 10$ )

$E_1/E_2$	Present	LWT <sup>1</sup>	TOT <sup>2</sup>	RFT	Present DQ results		
					P = 3(TOT)	P = 7	P = 5
2	2.47209	2.4672	2.4721	2.4721	2.4721	2.4771	2.4744
5	4.7728	4.6703	4.7728	4.7728	4.7728	4.7928	4.7823
10	8.53874	8.1229	8.5390	8.5386	8.5390	8.6029	8.5697
15	12.3511	11.5069	12.3517	12.3509	12.3517	12.4799	12.4134
20	16.3081	14.9536	16.3091	16.3076	16.3090	16.5195	16.4099
30	25.0718	22.4823	25.0733	25.0700	25.0733	25.5007	25.2756

Table 11 Continued

$E_1/E_2$	Present	LWT <sup>1</sup>	TOT <sup>2</sup>	RFT	Present DQ results		
					GRT (9x9)		
					P = 3(TOT)	P = 7	P = 5
40	35.90239	31.7113	35.9042	35.8980	35.9041	36.6308	36.2438
50	50.68244	44.2904	50.6840	50.6737	50.6840	51.8351	51.2138

<sup>1</sup>Cetkovic (2016), <sup>2</sup>Matsunaga (2005)

Table 12 Effects of the thermal expansion coefficients ratio on the dimensionless buckling temperature ( $T_{cr} = T\alpha_0 10^3$ ) of the square simply supported antisymmetric angle-ply  $(45/-45)_3$  plates ( $a/h = 10$ )

$\alpha_2/\alpha_1$	Present	LWT <sup>1</sup>	TOT <sup>2</sup>	RFT	Present DQ results		
					RFT		
					P = 3(TOT)	P = 7	P = 5
1	10.3861	9.3134	10.3868	10.3854	10.3867	10.4707	10.5638
5	8.99978	8.0703	9.0003	8.9991	9.0003	9.0730	9.1537
10	7.71288	6.9163	7.7134	7.7123	7.7133	7.7757	7.8448
20	5.99765	5.3782	5.9980	5.9972	5.9980	6.0465	6.1002
30	4.9065	4.3998	4.9068	4.9062	4.9068	4.9464	4.9904
40	4.1513	3.7225	4.1515	4.1510	4.1515	4.1851	4.2223
50	3.5975	3.2260	3.5978	3.5973	3.5977	3.6268	3.6591
1	10.3861	9.3134	10.3868	10.3854	10.3867	10.4707	10.5638

<sup>1</sup>Cetkovic (2016), <sup>2</sup>Matsunaga (2005)

Table 10 show another comparison with, Chen and Liu,1993, for antisymmetric laminated square thick plate ( $a/h = 10$ ) for different aspect ratio ( $b/a$ ), angle orientation (30, 45 and 60) and number of layer (2, 4 and 8) which give closed results with maximum discrepancy (2.28 %). Material constant given as:

Material 6:  $\frac{E_1}{E_2} = 25, G_{12} = G_{13} = 0.5 E_2, G_{23} = 0.2E_2, \nu_{12} = 0.25, \alpha_2/\alpha_1 = 3$

Table 11 show the effect of changing ( $E_1/E_2$ ) on critical temperature for six layers of antisymmetric angle-ply  $(45/-45)_3$  plates for thickness ratio ( $a/h = 10$ ) since stiffness increase when increasing orthotropic ratio, therefore normalized critical temperature increase. Material constants are given as:

Material 7:  $\frac{E_1}{E_2} = open, \frac{E_2}{E_0} = 1, \frac{G_{12}}{E_0} = \frac{G_{13}}{E_0} = 0.65, \frac{G_{23}}{E_0} = 0.639, \nu_{12} = 0.21, \frac{\alpha_1}{\alpha_0} = -0.21, \frac{\alpha_2}{\alpha_0} = 16, E_0 = 10Gpa, \alpha_0 = 10^{-6}$

Table 12. show the effect of changing  $\alpha_2/\alpha_1$  on critical temperature for six layers of antisymmetric angle-ply  $(45/-45)_3$  plates for thickness ratio ( $a/h = 10$ ) since stiffness decrease, when thermal expansion coefficient ratio increase therefore normalized critical temperature decrease. Material constants are given as:

Material 8:  $\frac{E_1}{E_0} = 30, \frac{E_2}{E_0} = 1, \frac{G_{12}}{E_0} = \frac{G_{13}}{E_0} = 0.65, \frac{G_{23}}{E_0} = 0.639, \nu_{12} = 0.21, \frac{\alpha_1}{\alpha_0} = 1, \frac{\alpha_2}{\alpha_1} = open, E_0 = 10Gpa$

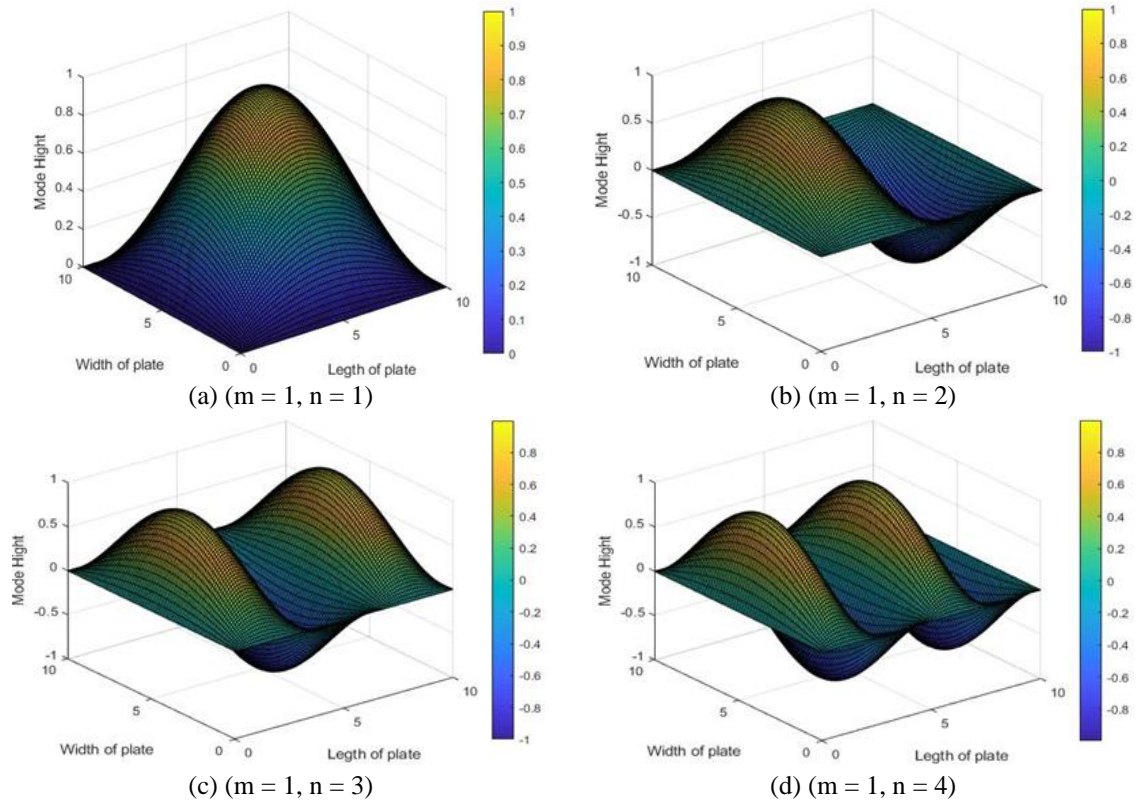


Fig. 3 Thermal buckling mode for antisymmetric angle-ply square plate, No. of layers = 4,  $a/h = 10$ ,  $a/b = 2$

Figs. 3(a)-3(d) shows first four buckling mode of angle-ply moderately thick plate ( $a/h = 10$ ) rectangular ( $a/b = 2$ ) simply supported laminated plate.

## 5. Conclusions

The following conclusions may be derived:

- The most important characteristic of this work is that it contains five unknown displacement of refined plate theory, which compared with other theories those of the refined four parameters plate theory (RPT), FSDT, HSDT, LWT and Noor, 1992 and give good agreement.
- The critical temperature buckling is affected by design parameters (aspect ratio ( $a/bh$ ), thickness ratio ( $a/h$ ), lamination angle, modulus elastically ratio ( $E_1/E_2$ ) and thermal expansion coefficient ratio ( $\alpha_1/\alpha_2$ )).
- The critical buckling temperature depend on the lamination scheme, especially for thick laminates and is greater for  $[0/90/0]$ , compared to  $[0/90]$  laminates, when the same material properties of each layer are used.
- The critical buckling temperature decreases with the increase of modulus ratio  $E_1/E_2$ , this decreasing for only cross-ply plate.
- The critical buckling temperature increases with the increase of modulus ratio  $E_1/E_2$  for angle-ply plate

- The critical buckling temperature decreases with the increase of thermal expansion coefficient ratio ( $\alpha_2/\alpha_1$ ) and is faster for thick, compared to thin laminates.
- The critical buckling temperature increases with the increase of aspect ratio  $a/b$ . This increase is again more pronounced for thick, compared to thin laminates. For  $a/b > 2$  the increase of critical temperature is almost linear, and thus the same for all buckling mode shapes.
- For the same materials, angle-ply has a greater critical temperature buckling than cross-ply.

## Acknowledgments

The research described in this paper was financially supported by the Natural Science Foundation.

## References

- Abdul-Majeed, W.R., Jweeg, M.J., and Jameel, A.P.D.A.N. (2011), "Thermal buckling of rectangular plates with different temperature distribution using strain energy method", *J. Eng.*, **17**(5), 1047-1065.
- Abdul, Z.A.K. and Majeed, W.I. (2020), "Effect of boundary conditions on harmonic response of laminated plates", *Compos. Mater. Eng.*, **2**(2), 125-140. <http://doi.org/10.12989/cme.2020.2.2.125>.
- Abualnour, M., Chikh, A., Hebali, H., Kaci, A., Tounsi, A., Bousahla, A.A. and Tounsi, A. (2019), "Thermomechanical analysis of antisymmetric laminated reinforced composite plates using a new four variable trigonometric refined plate theory", *Comput. Concrete*, **24**(6), 489-498. <https://doi.org/10.12989/cac.2019.24.6.489>.
- Bakoura, A., Bourada, F., Bousahla, A.A., Tounsi, A., Benrahou, K.H., Tounsi, A., Al-Zahrani, M.M. and Mahmoud, S.R. (2021), "Buckling analysis of functionally graded plates using HSDT in conjunction with the stress function method", *Comput. Concrete*, **27**(1), 73-83, <https://doi.org/10.12989/cac.2021.27.1.073>.
- Belbachir, N., Draich, K., Bousahla, A.A., Bourada, M., Tounsi, A. and Mohammadimehr, M. (2019), "Bending analysis of antisymmetric cross-ply laminated plates under nonlinear thermal and mechanical loadings", *Steel Compos. Struct.*, **33**(1), 81-92. <http://doi.org/10.12989/scs.2019.33.1.081>.
- Belbachir, N., Bourada, M., Draiche, K., Tounsi, A., Bourada, F., Bousahla, A.A. and Mahmoud, S.R. (2020), "Thermal flexural analysis of anti-symmetric cross-ply laminated plates using a four variable refined theory", *Smart Struct. Syst.*, **25**(4), 409-422, <https://doi.org/10.12989/sss.2020.25.4.409>.
- Bensaid, I., Bekhadda, A. and Kerboua, B. (2021), "Size-dependent bending and stability analysis of FG nano-beams via a novel simplified first-order shear deformation beam theory", *Compos. Mater. Eng.*, **3**(1), 71-88. <https://doi.org/10.12989/cme.2021.3.1.071>.
- Bourada, M., Tounsi, A., Houari, M.S.A. and Bedia, E.A. A. (2012), "A new four-variable refined plate theory for thermal buckling analysis of functionally graded sandwich plates", *J. Sandw. Struct. Mater.*, **14**(1), 5-33. <https://doi.org/10.1177/2F1099636211426386>.
- Cetkovic, M. (2016), "Thermal buckling of laminated composite plates using layerwise displacement model", *Compos. Struct.*, **142**(10), 238-253. <https://doi.org/10.1016/j.compstruct.2016.01.082>.
- Chang, J.S. and Leu, S.Y. (1991), "Thermal buckling analysis of antisymmetric angle-ply laminates based on a higher-order displacement field", *Compos. Sci. Technol.*, **41**(2) 109-128. [https://doi.org/10.1016/0266-3538\(91\)90023-I](https://doi.org/10.1016/0266-3538(91)90023-I).
- Chen, W.J., Lin, F.D. and Chen, L.W. (1991), "Thermal buckling behavior of thick composite laminated plates under nonuniform temperature distribution", *Comput. Struct.*, **41**(4), 637-645. [https://doi.org/10.1016/0045-7949\(91\)90176-M](https://doi.org/10.1016/0045-7949(91)90176-M).
- Chikr, S.C., Kaci, A., Bousahla, A.A., Bourada, F., Tounsi, A., Bedia, E.A.A., Mahmoud, S.R., Benrahou, K.H., Tounsi, A. (2020), "A novel four-unknown integral model for buckling response of FG sandwich plates resting on elastic foundations under various boundary conditions using Galerkin's approach",

- Geomech. Eng.*, **21**(5), 471-487. <https://doi.org/10.12989/gae.2020.21.5.471>.
- Ghadimi, M.G. (2020), "Buckling of non-sway Euler composite frame with semi-rigid connection", *Compos. Mater. Eng.*, **2**(1), 13-24. <http://doi.org/10.12989/cme.2020.2.1.013>.
- Hussein, E. and Alasadi, S. (2018), "Experimental and theoretical stress analysis investigation for composite plate under thermal load", *Kufa J. Eng.*, **9**(1), 205-221. <http://doi.org/10.30572/2018/KJE/090114>.
- Jameel, A.N. (2013), "Buckling analysis of composite plates under thermo-mechanical loading", *Al-Rafidain Univ. Coll. Sci.*, (32).
- Kim, S.E., Thai, H.T. and Lee, J. (2009), "A two variable refined plate theory for laminated composite plates", *Compos. Struct.*, **89**(2), 197-205. <https://doi.org/10.1016/j.compstruct.2008.07.017>.
- Kumar, J. and Gupta, A. (2014), "Thermal buckling of symmetric cross-ply laminated plate", *Int. J. Sci. Res.*, **3**(6), 2488 - 2491. <http://doi.org/10.32628/ijrsrset207436>.
- Kumar, R., Sharma, A. and Kumar, R. (2013), "Thermal buckling analysis of a laminated composite plate resting on elastic foundation using Stochastic finite element method based on micromechanical model", *Int. J. Business Enterprise Appl.*
- Matsunaga, H. (2006), "Thermal buckling of angle-ply laminated composite and sandwich plates according to a global higher-order deformation theory", *Compos. Struct.*, **72**(2), 177-192. <https://doi.org/10.1016/j.compstruct.2004.11.016>.
- Menasria, A., Kaci, A., Bousahla, A.A., Bourada, F., Tounsi, A., Adda Bedia, E.A. and Mahmoud, S.R. (2020), "A four-unknown refined plate theory for dynamic analysis of FG-sandwich plates under Various boundary conditions", *Steel Compos. Struct.*, **36**(3), 355-367. <http://doi.org/10.12989/scs.2020.36.3.355>.
- Noor, K. and Scott, B.W. (1992), "Three-dimensional solutions for the thermal buckling and sensitivity derivatives of temperature-sensitive multilayered angle-ply plates", *J. Appl. Mech T.*, **59**(4). <https://doi.org/10.1115/1.2894052>.
- Ounis, H. and Belarbi, M.-O. (2017), "On the thermal buckling behaviour of laminated composite plates with cut-outs", *J. Appl. Eng. Sci. Technol.*, **3**(2), 63-69.
- Prabhu, M. R. and Dhanaraj, R. (1994), "Thermal buckling of laminated composite plates", *Comput. Struct.*, **53**(5), 1193-1204. <https://doi.org/10.1080/01495738708927017>.
- Reddy, J.N (2004), *Mechanics of Laminated Composite Plates and Shells Theory Analysis*, CRC Press, Boca Raton, Florida, U.S.A.
- Sadiq, I.A. and Majeed, W.I., "Thermal buckling of angle-ply laminated plates using new displacement function", *J. Eng.*, **25**(12), 96-113. <http://doi.org/10.31026/j.eng.2019.12.08>.
- Shu, X. and Sun, L. (1994), "Thermomechanical buckling of laminated composite plates with higher-order transverse shear deformation", *Comput. Struct.*, **53**(1), 1-7. <https://doi.org/10.1016/0045-7949/2894/2990123-6>
- Singh, R.K. (2014), "Thermal buckling analysis of laminated composite shell panel embedded with shape memory alloy fibre under TD and TID", MTech thesis, National Institute of Technology Rourkela, Rourkela, India.
- Tahir, S.I., Chikh, A., Tounsi, A., Al-Osta, M.A., Al-Dulaijan, S.U. and Al-Zahrani, M.M. (2021), "Wave propagation analysis of a ceramic-metal functionally graded sandwich plate with different porosity distributions in a hygro-thermal environment", *Compos. Struct.*, **269**, 114030. <https://doi.org/10.1016/j.compstruct.2021.114030>.
- Thangaratnam, K.R. and Ramachandran, J. (1989), "Thermal buckling of composite laminated plates", *Comput. Struct.*, **32**(5), 1117-1124. [https://doi.org/10.1016/0045-7949\(89\)90413-6](https://doi.org/10.1016/0045-7949(89)90413-6).
- Tounsi, A., Atmane, H.A., Khiloun, M., Sekkal, M., Taleb, O. and Bousahla, A.A. (2019), "On buckling behavior of thick advanced composite sandwich plates", *Compos. Mater. Eng.*, **1**(1), 1-19, <http://doi.org/10.12989/cme.2019.1.1.001>.
- Xing, Y. and Wang, Z. (2017), "Closed form solutions for thermal buckling of functionally graded rectangular thin plates", *Appl. Sci.*, **7**(12), 1256. <http://doi.org/10.3390/app7121256>.

## Appendix

For stiffness cross-ply:

$$\begin{aligned}
 s_{11} &= A_{11}\alpha^2 + A_{66}\beta^2, \quad s_{12} = (A_{12} + A_{66})\alpha\beta, \quad s_{13} = -B_{11}\alpha^3 - (B_{12} + 2B_{66})\alpha\beta^2, \\
 s_{14} &= -B_{11}^s\alpha^3 - (B_{12}^s + 2B_{66}^s)\alpha, \quad s_{22} = A_{66}\alpha^2 + A_{22}\beta^2, \quad s_{23} = -(B_{12} + 2B_{66})\alpha^2\beta - B_{22}\beta^3, \\
 s_{24} &= -(B_{12}^s + 2B_{66}^s)\alpha^2\beta - B_{22}^s\beta^3, \quad s_{33} = D_{11}\alpha^4 + 2(D_{12} + 2D_{66})\alpha^2\beta^2 + D_{22}\beta^4, \\
 s_{34} &= D_{11}^s\alpha^4 + 2(D_{12}^s + 2D_{66}^s)\alpha^2\beta^2 + D_{22}^s\beta^4, \quad s_{44} = H_{11}^s\alpha^4 + 2(H_{12}^s + 2H_{66}^s)\alpha^2\beta^2 + H_{22}^s\beta^4 \\
 &\quad + A_{55}^s\alpha^2 + A_{44}^s\beta^2, \quad s_{45} = A_{55}^a\alpha^2 + A_{44}^a\beta^2, \quad s_{55} = A_{55}\alpha^2 + A_{44}\beta^2 \\
 A_{16} &= A_{26} = D_{16} = D_{26} = D_{16}^s = D_{26}^s = H_{16}^s = H_{26}^s = B_{16} = B_{26} = B_{12}^s = B_{16}^s = B_{26}^s = A_{45} \\
 &= A_{45}^a = A_{45}^s = 0
 \end{aligned}$$

For stiffness angle-ply:

$$\begin{aligned}
 s_{11} &= A_{11}\alpha^2 + A_{66}\beta^2, \quad s_{12} = (A_{12} + A_{66})\alpha\beta, \quad s_{13} = -(3B_{16}\alpha^2\beta + B_{26}\beta^3), \\
 s_{14} &= -(3B_{16}^s\alpha^2\beta + B_{26}^s)\beta^3, \quad s_{22} = A_{66}\alpha^2 + A_{22}\beta^2, \quad s_{23} = -(B_{16}\alpha^3 + 3B_{26}\alpha\beta^2), \\
 s_{24} &= -(B_{16}^s\alpha^3 + 3B_{26}^s\alpha\beta^2), \quad s_{33} = D_{11}\alpha^4 + 2(D_{12} + 2D_{66})\alpha^2\beta^2 + D_{22}\beta^4, \\
 s_{34} &= D_{11}^s\alpha^4 + 2(D_{12}^s + 2D_{66}^s)\alpha^2\beta^2 + D_{22}^s\beta^4, \\
 s_{44} &= H_{11}^s\alpha^4 + 2(H_{12}^s + 2H_{66}^s)\alpha^2\beta^2 + H_{22}^s\beta^4 + A_{55}^s\alpha^2 + A_{44}^s\beta^2, \\
 s_{45} &= A_{55}^a\alpha^2 + A_{44}^a\beta^2, \quad s_{55} = A_{55}\alpha^2 + A_{44}\beta^2 \\
 A_{16} &= A_{26} = D_{16} = D_{26} = D_{16}^s = D_{26}^s = H_{16} = H_{26} = H_{16}^s = H_{26}^s = B_{11} = B_{12} = B_{22} = B_{66} = B_{11}^s \\
 &= B_{12}^s = B_{22}^s = B_{66}^s = 0 \\
 A_{45} &= A_{45}^a = A_{45}^s = 0
 \end{aligned}$$

The plane stress reduced stiffness  $Q_{ij}$  are Reddy (2004)

$$\begin{aligned}
 Q_{11} &= \frac{E_1}{1-\nu_{12}\nu_{21}}, \quad Q_{12} = \frac{\nu_{12}E_2}{1-\nu_{12}\nu_{21}}, \quad Q_{11} = \frac{E_2}{1-\nu_{12}\nu_{21}}, \quad Q_{66} = G_{12}, \quad Q_{44} = G_{23}, \quad Q_{55} = G_{13} \\
 \alpha &= \frac{m\pi}{a}, \quad \beta = \frac{m\pi}{b}, \quad \text{and } (U_{mn}, V_{mn}, W_{bmn}, W_{bmn}, W_{bmn}) \text{ are coefficients}
 \end{aligned}$$